In the second experiment, we consider the transmission of voice and data traffic over PCF. In this experiment, eight nodes are polled by the PC, where nodes 1 to 4 transmit voice traffic [13] and nodes 5 to 8 transmit data traffic at a rate of 11 Mb/s (i.e., $R_{\mathrm{data}} = 11$ Mb/s), and each node takes a different parameter setting shown in Table II. Fig. 5(a) plots the mean total delay per data frame [i.e., (4) and (17)] for each node, and Fig. 5(b) plots the corresponding standard deviation [i.e., (3)], where the abscissa represents the node ID, the bar with dashed border represents the simulation results, and the bar with solid border represents the theoretical results. Note that the standard deviation of the total delay is same to that of the waiting delay since $U_i$ in (4) is a constant. In Figs. 5(a) and (b), each node has an apparently different mean delay and delay variance since each node takes a very different parameter setting. The close match between the theoretical curves and the corresponding simulation curves manifests that our theoretical results are very accurate for heterogeneous traffic as well.

## VI. Conclusion

The IEEE 802.11 PCF network is a polling-based system. This paper has proposed using the $M/G/1$ vacation model to analyze the delay performance of the PCF. Our method is powerful and scalable. This paper lays a solid foundation to analyze the variants of the PCF protocol such as 802.11e HCCA and 802.16.

## Acknowledgment

The authors would like to thank the anonymous reviewers for their helpful suggestions and insightful comments on this paper.

## References

[1] *Part 11: Wireless LAN Medium Access Control (MAC) and Physical Layer (PHY) Specifications*, ANSI/IEEE Std. 802.11, 1999.
[2] B. Sikdar, "An analytic model for the delay in IEEE 802.11 PCF MAC-based wireless networks," *IEEE Trans. Wireless Commun.*, vol. 6, no. 4, pp. 1542–1550, Apr. 2007.
[3] M. Visser and M. El Zarki, "Voice and data transmission over an 802.11 wireless network," in *Proc. IEEE PIMRC*, 1995, pp. 648–652.
[4] J. Wu and G. Huang, "Simulation study based on qos schemes for IEEE 802.11," in *Proc. 3rd ICACTE*, Aug. 2010, pp. 534–538.
[5] M. Siddique and J. Kamruzzaman, "Performance analysis of PCF based WLANS with imperfect channel and failure retries," in *Proc. IEEE GLOBECOM*, Dec. 2010, pp. 1–6.
[6] Q. Liu and D. Zhao, "Analysis of two-level-polling system with mixed access policies," in *Proc. ICICTA*, Oct. 2009, pp. 357–360.
[7] H. Ding, D. Zhao, and Y. Zhao, "Analysis of polling system with multiple vacations and using exhaustive service," in *Proc. Asia-Pacific Conf. CICC-ITOE*, Jan. 2010, pp. 294–296.
[8] B. Sikdar, "Queueing analysis of polled service classes in the IEEE 802.16 MAC protocol," *IEEE Trans. Wireless Commun.*, vol. 8, no. 12, pp. 5767–5772, Dec. 2009.
[9] H. Yang and B. Sikdar, "Queueing analysis of polling based wireless MAC protocols with sleep-wake cycles," *IEEE Trans. Commun.*, vol. 60, no. 9, pp. 2427–2433, Sep. 2012.
[10] R. Iyengar and B. Sikdar, "A queueing model for polled service in WiMAX/IEEE 802.16 networks," *IEEE Trans. Commun.*, vol. 60, no. 7, pp. 1777–1781, Jul. 2012.
[11] D. P. Bertsekas and R. Gallager, *Data Networks*. Englewood Cliffs, NJ, USA: Prentice-Hall, 1992, pp. 192–195.
[12] H. Takagi, Queueing Analysis, vol. 1, Amsterdam, The Netherlands: North-Holland 1991.
[13] L. X. Cai, X. Shen, J. Mark, L. Cai, and Y. Xiao, "Voice capacity analysis of wlan with unbalanced traffic," *IEEE Trans. Veh. Technol.*, vol. 55, no. 3, pp. 752–761, May 2006.
[14] C. Cicconetti, L. Lenzini, E. Mingozzi, and G. Stea, "A software architecture for simulating IEEE 802.11e HCCA," in *Proc. 3rd IPS-MoMe*, Mar. 14/15, 2005, pp. 97–104.

# A Multidimensional Resource-Allocation Optimization Algorithm for the Network-Coding-Based Multiple-Access Relay Channels in OFDM Systems

Bin Han, Mugen Peng, *Senior Member, IEEE*, Zhongyuan Zhao, and Wenbo Wang, *Member, IEEE*

***Abstract*—Joint scheduling and resource allocation in uplink orthogonal frequency-division multiplexing (OFDM) systems is complicated and even becomes intractable with a large subcarrier and a large user number. This paper investigates the resource allocation for OFDM-based multiuser multiple-access relay channels (MARCs) with network coding. We formulate a joint optimization problem considering source-node pairing, subcarrier assignment, subcarrier pairing, and power allocation to maximize the sum rate under per-user power constraints. The problem is solved in polynomial time by optimizing three separate subproblems. To further reduce the complexity, three low-complexity suboptimal algorithms are then proposed when fixing partial resource. The simulation results show the performance gains of the proposed algorithms versus per-node transmit power and source-node number, and the impact of relay location is also evaluated.**

***Index Terms*—Multiple-access relay channels (MARC), network coding, orthogonal frequency-division multiplexing (OFDM), resource allocation.**

## I. Introduction

Wireless relays can provide reliable transmission and broad coverage for next-generation wireless networks [1], [2]. The relay node assists transmission by forwarding messages from a source to a destination, where several cooperative protocols were introduced, including amplify-and-forward (AF) and decode-and-forward (DF) schemes [2]. However, such relay is always assumed to be half-duplex so that the spectral efficiency suffers from an inherent loss. To overcome this shortcoming, network coding, which was originally proposed in wired communications, can be applied in relay systems [3]–[5].

Recently, many novel protocols have been studied in multiple-access relay channels (MARCs) with network coding, where multiple sources send wireless symbols to a destination with the help of a network-coded relay, such as the DF-based protocol in [6] and [10]–[12] and the AF-based protocol in [7]. A typical MARC consists of two sources, a relay, and a destination. As depicted in Fig. 1(a), the conventional way requires four stages to accomplish transmission. Since the destination can receive messages from the source and the relay, this transmission protocol can achieve a diversity order of 2. However,

Manuscript received April 24, 2012; revised September 12, 2012 and January 10, 2013; accepted February 19, 2013. Date of publication March 7, 2013; date of current version October 12, 2013. This work was supported in part by the National Natural Science Foundation of China under Grant 61222103, by the National Basic Research Program of China under Grant 2013CB336600, by the State Major Science and Technology Special Projects under Grant 2010ZX03003-003-01, by the Beijing Natural Science Foundation under Grant 4131003, by the Specialized Research Fund for the Doctoral Program of Higher Education and the Research Grants Council Earmarked Research Grants under Grant 20120005140002, and by the Program for New Century Excellent Talents in University. This paper was presented in part at the IEEE Global Communications Conference, Anaheim, CA, USA, December 3–7, 2012. The review of this paper was coordinated by Prof. Y. Su.

The authors are with the Key Laboratory of Universal Wireless Communications for Ministry of Education, Beijing University of Posts and Telecommunications, Beijing 100876, China (e-mail: hanbin.jason@gmail.com; pmg@bupt.edu.cn; zhaozhongyuan0323@gmail.com; wbwang@bupt.edu.cn).

Color versions of one or more of the figures in this paper are available online at http://ieeexplore.ieee.org.

Digital Object Identifier 10.1109/TVT.2013.2251025

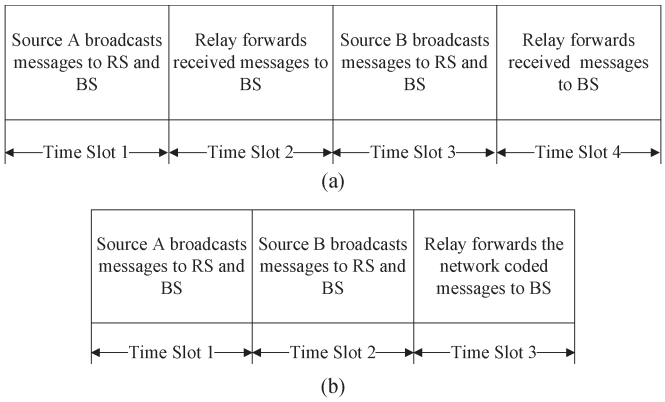


Fig. 1. Frame structure for conventional cooperative and network-coded cooperative MARCs. (a) Frame structure for the conventional cooperative MARC. (b) Frame structure for the cooperative MARC with network coding.

the network-coded cooperative protocol, as depicted in Fig. 1(b), only requires three stages and therefore becomes more efficient. In this transmission protocol, the relay forwards the network-coded message, instead of two separate messages, which still achieves full cooperative diversity. In [6], a new framework termed adaptive DF-based network-coded cooperation was proposed, where the achievable rates and outage probabilities were evaluated. Ding *et al.* [7] discussed the outage probability and diversity gain for a network-coded cooperative MARC and showed that the proposed AF-based protocol can achieve transmission of two sources to a destination within two stages. However, this protocol does rely on the assumption of precise time synchronization both on the relay and the destination at the first stage. Note that, after the signals traverse the wireless channel, there is a phase shift that depends on the distance between the sender and the receiver. Since the phase shifts are different from the two sources to the relay and the destination, respectively, therefore, the perfect synchronization is not feasible. In this paper, we consider a three-stage AF-based protocol, which is similar to the time-division broadcast protocol in [8] and [9]. Although we do need time synchronization in this protocol, the received signals will be synchronized separately, which is more feasible in practice. To further improve performance for the future generation of wireless systems, a MARC with network coding has been studied jointly with other transmission technologies, such as multiple-input multiple-output (MIMO) [11] and orthogonal frequency-division multiplexing (OFDM) [12].

On the other hand, efficient resource allocation is critical to improve performance in wireless communication systems. Several resource-allocation schemes for OFDM-based conventional one-way relay networks have been proposed in [13]–[15]. In [13], Kaneko *et al.* investigated a *subcarrier-fixed* resource-allocation scheme in two-hop relay networks. Here, subcarrier fixed indicates that signals received at a relay node from one subcarrier are broadcasted over the same subcarrier in the next hop. It can be observed that such a scheme does not fully utilize the differences of channel conditions. Thus, better performance could be achieved if the subcarriers between two phases are paired, which is known as *subcarrier pairing*. Li *et al.* [14] studied the subcarrier pairing and power allocation in AF and DF OFDM relay systems. In [15], Dang *et al.* proposed a framework for joint optimization of power and subcarrier allocation, relay selection, and subcarrier pairing for single-user multiple one-way OFDM systems. Motivated by the previous works in two-hop one-way relay networks, several resource-allocation schemes for network-coded two-way relay system have been studied, which can improve spectral efficiency [17]–[19]. Ho *et al.* [17] studied subcarrier pairing and power allocation in three-node two-way relay channels, where they did not involve source pairing and subcarrier assignment. In [18], the subcarrier-pairing-based resource allocation considering subcarrier assignments and relay selection was investigated in OFDM-based multiuser two-way relay networks, where the authors did not consider power allocation for simplicity. However, per-node power constraints make the problem even less tractable. Zhang *et al.* [19] studied the joint optimization problem of subcarrier-pairing-based relay power allocation, relay selection, and subcarrier assignment, whereas source pairing was not taken into account. However, to the best of the authors' knowledge, resource allocation jointly optimizing source-node pairing, subcarrier assignment, subcarrier pairing, and power allocation in OFDM-based MARCs with network coding has not been addressed in the literature.

In this paper, a joint optimization problem of maximizing the sum rate by varying source-node pairing, subcarrier assignment, subcarrier pairing, and power allocation is studied in OFDM-based network-coded MARC with the help of an AF relay. The main contributions of this paper are summarized as follows.

1) A new optimization problem where all the resources are jointly optimized is formulated for OFDM-based network-coded MARCs with the help of an AF relay. Unlike many previous works on resource allocation in OFDM one-way relay networks [13]–[15], this problem considers network coding technology. Different from previous works in two-way relay systems [16]–[20], intrapair interference (self-interference) can be subtracted at source receivers in two-way relay channels, whereas in network-coded MARCs, the intrapair interference cannot be completely eliminated. This interference makes source pairing and subcarrier allocation more complicated than that in two-way relay channels. Hence, the resource allocation in network-coded MARC is much different from that in two-way relay channels, and as a result, the schemes proposed in [16]–[20] cannot be extended to apply in this paper.
2) To solve this optimization problem, we must overcome three major challenges. First, resource allocation for OFDM systems is usually a mixed-integer-programming problem with exponential computational complexity. Second, in uplink network-coded MARCs, the individual-user power constraints and intrauser interference in each user pair make this problem more intractable. Third, power allocation, subcarrier assignment, and subcarrier pairing are tightly coupled, i.e., different subcarrier assignments lead to different subcarrier pairing and power allocation. Therefore, we solve the problem through three phases, and the complexity of proposed resource-allocation algorithm is polynomial with the number of subcarriers and source nodes.
3) Based on the optimization framework proposed in this paper, we further propose three low-complexity algorithms when fixing partial resource among subcarrier assignment, subcarrier pairing, and transmit power, and then evaluate the performance loss by simulations.

The rest of this paper is organized as follows. Section II provides the detail of the system model and formulates the resource-allocation problem. In Section III, the proposed resource-allocation algorithm is given by solving three separate subproblems. Section IV presents three low-complexity algorithms and provides simulation results to show the performance of the proposed algorithms. Finally, Section V concludes this paper.

*Notation:* Scalars are denoted by lowercase letters, e.g., $x$; boldface lowercase letters are used for vectors, e.g., $\mathbf{x}$; and boldface uppercase letters are used for matrices, e.g., $\mathbf{X}$. $\mathbb{E}(x)$ is the expectation of various $x$. $|x|$ denotes the norm of complex number $x$. $(x)^+$ denotes the maximum between a real number $x$ and zero. $\mathbf{X}^*$, $\mathbf{X}^T$, and $\mathbf{X}^H$ denote conjugate, transpose, and conjugate transpose, respectively.

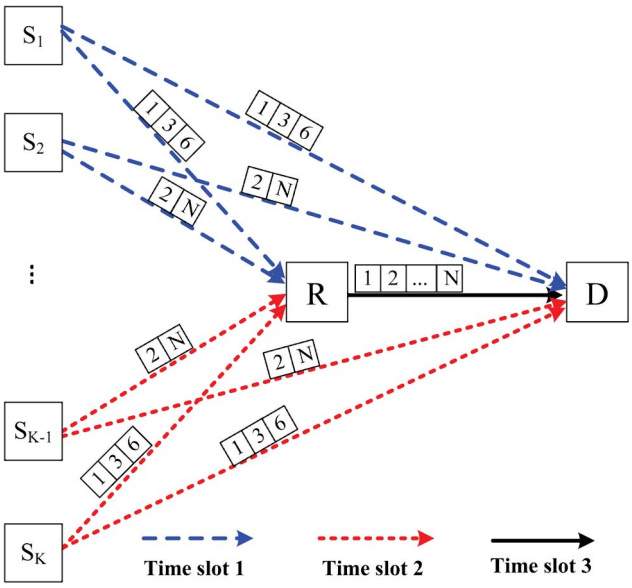


Fig. 2. System model for the OFDM-based network-coded MARC.

## II. System Model

Consider a network-coded MARC (see Fig. 2), where $K$ source nodes, which are denoted by $S_1, S_2, \ldots, S_K$, transmit information to destination $D$ with the help of AF-based relay node $R$. The transmission is based on OFDM technology; thus, each channel is logically divided into $N$ subcarriers. We assume that each node can acquire the complete channel knowledge through training or preambles, and perfect synchronization has been established among all the nodes prior to data transmission.

### A. MARC With Network Coding

For the source pair $(k, \varphi_k)$, we denote two source nodes as $S_k$ and $S_{\varphi_k}$, respectively. In each transmission frame, three time slots are applied for a source pair to communicate with a destination through network coding [see Fig. 1(b)].

*1) Broadcast Phase:* In the broadcast phase, each source node broadcasts its symbols in turn. At the first time slot, $S_k$ sends signals on subcarrier $n$. The received signals at $D$ and $R$ can be expressed, respectively, as

$$y_{kD}^n = \sqrt{p_k^n} h_{kD}^n x_k^n + n_D^n \tag{1}$$

$$y_{kR}^n = \sqrt{p_k^n} h_{kR}^n x_k^n + n_R^n \tag{2}$$

where $x_k^n$ is the transmitted symbol with unit power from source node $S_k$, $p_k^n$ is the transmit power for $S_k$ on subcarrier $n$, and $n_D^n$ and $n_R^n$ are the additive white Gaussian noise at $D$ and $R$, respectively (i.e., $\mathbb{E}(n_D^n) = \sigma_{D^n}^2$ and $\mathbb{E}(n_R^n) = \sigma_{R^n}^2$). The channel coefficients from $S_k$ to destination $D$ (relay $R$) on subcarrier $n$ is denoted by $h_{kD}^n (h_{kR}^n)$.

At the second time slot, the source node $S_{\varphi_k}$, which is paired with $S_k$, sends signal on subcarrier $n$. Similarly, the received signals at $D$ and $R$ can be written, respectively, as

$$y_{\varphi_k D}^n = \sqrt{p_{\varphi_k}^n} h_{\varphi_k D}^n x_{\varphi_k}^n + n_D^n \tag{3}$$

$$y_{\varphi_k R}^n = \sqrt{p_{\varphi_k}^n} h_{\varphi_k R}^n x_{\varphi_k}^n + n_R^n. \tag{4}$$

Here, $x_{\varphi_k}^n$ is the transmitted symbol with unit power from source node $S_{\varphi_k}$, $p_{\varphi_k}^n$ is the transmit power for $S_{\varphi_k}$ on subcarrier $n$, and $h_{\varphi_k D}^n (h_{\varphi_k R}^n)$ denotes channel coefficients from $S_{\varphi_k}$ to $D(R)$ on subcarrier $n$.

*2) Relay Phase:* At the third time slot, which is described as the relay phase, the relay amplifies the received signals from the previous two time slots and forwards them to node $D$ on subcarrier $\pi_n$. Therefore, node $D$ receives

$$y_{RD}^{\pi_n} = \sqrt{p_R^{\pi_n}} h_{RD}^{\pi_n} \left( \beta_1^n y_{kR}^n + \beta_2^n y_{\varphi_k R}^n \right) + n_D^{\pi^n} \tag{5}$$

where $p_R^{\pi_n}$ is the transmit power for relay $R$ on subcarrier $\pi_n$, $h_{RD}^{\pi_n}$ is the channel coefficient from $R$ to $D$, and $n_D^{\pi_n}$ is the additive white Gaussian noise at node $D$ on subcarrier $\pi_n$ (i.e., $\mathbb{E}(n_D^{\pi_n}) = \sigma_{D^{\pi_n}}^2$). Without loss of generality, in this paper, we assume $\sigma_{R^n}^2 = \sigma_{D^n}^2 = \sigma_{D^{\pi_n}}^2 = 1$. Here, $\beta_i^n$ is the amplification factor for time slot $i (i = 1, 2)$ and can be written as

$$\beta_1^n = \sqrt{\frac{\alpha_1^n}{p_k^n \left| h_{kR}^n \right|^2 + 1}} \approx \sqrt{\frac{\alpha_1^n}{p_k^n \left| h_{kR}^n \right|^2}} \tag{6}$$

$$\beta_2^n = \sqrt{\frac{\alpha_2^n}{p_{\varphi_k}^n \left| h_{\varphi_k R}^n \right|^2 + 1}} \approx \sqrt{\frac{\alpha_2^n}{p_{\varphi_k}^n \left| h_{\varphi_k R}^n \right|^2}} \tag{7}$$

where the approximation is based on the assumption that it is in the high-SNR region [14], [15]. To ensure that the transmit power of relay node is $P_R$, $\alpha_1^n$ and $\alpha_2^n$ should satisfy that $\alpha_1^n + \alpha_2^n = 1$.

Combining (1)–(5), the observations at destination $D$ can be expressed as

$$\mathbf{y} = \mathbf{H}\mathbf{x} + \mathbf{n} \tag{8}$$

where $\mathbf{x} = [x_k^n, x_{\varphi_k}^n]^T$, $\mathbf{y} = [y_{kD}^n, y_{\varphi_k D}^n, y_{RD}^{\pi_n}]^T$

$$\mathbf{H} = \begin{bmatrix} \sqrt{p_k^n} h_{kD}^n & 0 \\ 0 & \sqrt{p_{\varphi_k}^n} h_{\varphi_k D}^n \\ \sqrt{p_k^n p_R^{\pi_n}} \beta_1^n h_{RD}^{\pi_n} h_{kR}^n & \sqrt{p_{\varphi_k}^n p_R^{\pi_n}} \beta_2^n h_{RD}^{\pi_n} h_{\varphi_k R}^n \end{bmatrix}$$

$$\mathbf{n} = \begin{bmatrix} n_D^n \\ n_D^n \\ \left( \sqrt{p_R^{\pi_n}} \beta_1^n h_{RD}^{\pi_n} + \sqrt{p_R^{\pi_n}} \beta_2^n h_{RD}^{\pi_n} \right) n_R^n + n_D^{\pi_n} \end{bmatrix}.$$

Jiang *et al.* [21] have analyzed the performance of the zero-forcing (ZF) and MMSE equalizers in a MIMO system and presented the gains of the MMSE equalizer in a bit error rate and outage probabilities over the ZF equalizer. Therefore, in this paper, we consider MMSE equalizers. Based on the derivation in Appendix A, the output SNR for source $S_k$ and $S_{\varphi_k}$ can be expressed, respectively, as

$$\mathrm{SNR}_k^{n,\pi_n} = A + M - \frac{MN}{B + N + 1} \tag{9}$$

$$\mathrm{SNR}_{\varphi_k}^{n,\pi_n} = B + N - \frac{MN}{A + M + 1} \tag{10}$$

where $A = p_k^n |h_{kD}^n|^2$, $B = p_{\varphi_k}^n |h_{\varphi_k D}^n|^2$

$$M = \frac{\alpha_1 p_R^{\pi_n} \left| h_{RD}^{\pi_n} \right|^2}{\frac{\alpha_1 p_R^{\pi_n} \left| h_{RD}^{\pi_n} \right|^2}{p_k^n \left| h_{kR}^n \right|^2} + \frac{\alpha_2 p_R^{\pi_n} \left| h_{RD}^{\pi_n} \right|^2}{p_{\varphi_k}^n \left| h_{\varphi_k R}^n \right|^2} + 1}$$

$$N = \frac{\alpha_2 p_R^{\pi_n} \left| h_{RD}^{\pi_n} \right|^2}{\frac{\alpha_1 p_R^{\pi_n} \left| h_{RD}^{\pi_n} \right|^2}{p_k^n \left| h_{kR}^n \right|^2} + \frac{\alpha_2 p_R^{\pi_n} \left| h_{RD}^{\pi_n} \right|^2}{p_{\varphi_k}^n \left| h_{\varphi_k R}^n \right|^2} + 1}.$$

Again applying the high-SNR assumption, (9) and (10) can be rewritten as

$$\mathrm{SNR}_k^{n,\pi_n} \approx A + \frac{MB}{B+N} \tag{11}$$

$$\mathrm{SNR}_{\varphi_k}^{n,\pi_n} \approx B + \frac{NA}{A+M}. \tag{12}$$

For simplicity, we do not consider the power allocation between two data flows, and we assume that $\alpha_1^n = \alpha_2^n = 1/2$. Note that, in this case, we can obtain that $M = N$. Comparing $\mathrm{SNR}_k^{n,\pi_n}$ with $\mathrm{SNR}_{\varphi_k}^{n,\pi_n}$, it can be shown that

$$\begin{aligned}&\mathrm{SNR}_k^n - \mathrm{SNR}_{\varphi_k}^n \\ &\quad = (A-B)(AB+MA+MB)/\left((A+M)(B+M)\right) \\ &\qquad \times \begin{cases} >0, & A>B \\ =0, & A=B \\ <0, & A<B. \end{cases}\end{aligned} \tag{13}$$

Therefore, the achievable transmission rate (in nat/Hz) to the destination link for the source pair $(k, \varphi_k)$ on the subcarrier pair $(n, \pi_n)$ can be expressed as [21], [22]

$$\begin{aligned}C_{k,\varphi_k}^{n,\pi_n} &= C_k^{n,\pi_n} + C_{\varphi_k}^{n,\pi_n} \\ &= \frac{1}{3}\ln(1+\mathrm{SNR}_k^{n,\pi_n}) + \frac{1}{3}\ln(1+\mathrm{SNR}_{\varphi_k}^{n,\pi_n})\end{aligned} \tag{14}$$

where the factor of 1/3 accounts for three time slots in each transmission frame. We note that the standard Shannon capacity characterizes the maximal information rate supported in the channel with error-free transmission when the channel state information (CSI) is available at the transmitter, and optimal power allocation is adopted. However, in practice, the capacity is sacrificed not only from the suboptimal equalizers but also from other imperfect devices in the transceiver, such as the codec. In this paper, we only consider the transmission rate after using the MMSE equalizers and assume that the codec will be able to support a perfect error correction. Therefore, (14) describes the maximal supportable transmission rate after MMSE equalization.

### B. Problem Formulation

Let $\boldsymbol{\rho}$ be the resource-allocation indicator vector with elements $\rho_{k,\varphi_k}^{n,\pi_n} \in \{0,1\}$. When $\rho_{k,\varphi_k}^{n,\pi_n} = 1$, it indicates that subcarrier pair $(n,\pi_n)$ is allocated to source pair $(k,\varphi_k)$, and $\rho_{k,\varphi_k}^{n,\pi_n} = 0$ if otherwise. Define $\boldsymbol{\varphi} = [\varphi_1, \ldots, \varphi_K]$ as the source-node pairing vector, i.e., $S_{\varphi_k}$ is the pairing with source $S_k$. Let $\boldsymbol{\pi} = [\pi_1, \ldots, \pi_N]$ denote the subcarrier indicator vector, and the element $\pi_n$ indicates that the subcarrier $n$ in the broadcast phase pairs with subcarrier $\pi_n$ in the relay phase. To avoid interpair interference, variables $\boldsymbol{\pi}$ must satisfy that each subcarrier can be paired with only one subcarrier. We denote the transmit power vector as $\boldsymbol{p} = [p_k^1, \ldots p_k^N, p_R^1, \ldots p_R^N]$.

In this paper, our aim is to maximize the sum rate by optimizing $\boldsymbol{\rho}$, $\boldsymbol{\varphi}$, $\boldsymbol{\pi}$, and $\boldsymbol{p}$ under resource assignment and per-source power constraints. The optimization problem (Problem 2.1) can be formulated as follows:

$$\max_{\{\boldsymbol{\rho},\boldsymbol{\varphi},\boldsymbol{\pi},\boldsymbol{p}\}} \sum_{n=1}^{N}\sum_{k=1}^{K} 2\rho_{k,\varphi_k}^{n,\pi_n} C_k^{n,\pi_n} \tag{15}$$

$$\text{s.t.} \quad s_{k,\varphi_k}^{n,\pi_n} \le \min\{C_k, C_{\varphi_k}\} \le \phi_{k,\varphi_k}^{n,\pi_n} \quad \forall n,k \tag{16a}$$

$$\sum_{k=1}^{K} \rho_{k,\varphi_k}^{n,\pi_n} \le 1 \qquad \forall n \tag{16b}$$

$$\sum_{n=1}^{N} \rho_{k,\varphi_k}^{n,\pi_n} p_k^n \le P_k \qquad \forall k \tag{16c}$$

$$\sum_{n=1}^{N} p_R^{\pi_n} \le P_R. \tag{16d}$$

Here, $P_k$ and $P_R$ are the maximum transmit power of source node $k$ and relay node $R$, respectively. Here, $s_{k,\varphi_k}^{n,\pi_n}$ and $\phi_{k,\varphi_k}^{n,\pi_n}$ are the lower bound and upper bound transmission rate constraints, respectively, for source pair $(k,\varphi_k)$ on the subcarrier pair $(n,\pi_n)$, which can model scenarios when users have limited choices of modulation and coding schemes (MCSs). Constraint (16b) ensures that each subcarrier pair can only be allocated to one source pair. Equation (16c) and (16d) represent the source and relay power constraints, respectively.

Note that, at the optimum point, if we assume $C_k^{n,\pi_n{}^*} > C_{\varphi_k}^{n,\pi_n{}^*}$, then the optimum value can be denoted by $C_{\varphi_k}^{n,\pi_n{}^*} = \min\{C_k^{n,\pi_n{}^*}, C_{\varphi_k}^{n,\pi_n{}^*}\}$. Since $C_k^{n,\pi_n}$ increases with $p_k^n$ and $C_{\varphi_k}^{n,\pi_n}$ decreases with $p_k^n$, we can reduce $p_k^n$ such that $C_k^{n,\pi_n{}'} = C_{\varphi_k}^{n,\pi_n{}'}$. This reduction of $p_k^n$ will not violate the power constraints, and in this case, $C_{\varphi_k}^{n,\pi_n'} = \min\{C_k^{n,\pi_n\prime}, C_{\varphi_k}^{n,\pi_n}{}'\} > C_{\varphi_k}^{n,\pi_n^*}$. Therefore, at the optimum point, the first constraint can be rewritten as $C_k^{n,\pi_n} = C_{\varphi_k}^{n,\pi_n}$. Therefore, Problem 2.1 can be equivalently rewritten as (Problem 2.2) as follows:

$$\max_{\{\boldsymbol{\rho},\boldsymbol{\varphi},\boldsymbol{\pi},\boldsymbol{p}\}} \sum_{n=1}^{N}\sum_{k=1}^{K} 2\rho_{k,\varphi_k}^{n,\pi_n} C_k^{n,\pi_n} \tag{17}$$

$$\text{s.t.} \quad s_{k,\varphi_k}^{n,\pi_n} \le C_k^{n,\pi_n} = C_{\varphi_k}^{n,\pi_n} \le \phi_{k,\varphi_k}^{n,\pi_n} \tag{18a}$$

$$\sum_{k=1}^{K} \rho_{k,\varphi_k}^{n,\pi_n} \le 1 \quad \forall n \tag{18b}$$

$$\sum_{n=1}^{N} \rho_{k,\varphi_k}^{n,\pi_n} p_k^n \le P_k \quad \forall k \tag{18c}$$

$$\sum_{n=1}^{N} p_R^{\pi_n} \le P_R. \tag{18d}$$

Combining (13) with (18a), it can be observed that $p_k^n |h_{kD}^n|^2 = p_{\varphi_k}^n |h_{\varphi_k D}^n|^2$. It is worth noting that we can design the resource-allocation algorithm with fairness by easily rewriting the objective function in Problem 2.1 to a weighted sum rate.

## III. Optimal Resource Allocation

The joint optimization Problem 2.2 is a mixed-integer-programming problem and requires considerably high computational complexity. It is even intractable when $K$ and $N$ are very large. Here, we try to present a low-complexity and efficient solution by dividing the problem into three separate subproblems as follows.

- **P1:** Optimize the sum rate by varying source-node pairing $\boldsymbol{\varphi}$ and subcarrier assignment $\boldsymbol{\rho}$ when fixing power allocation $\boldsymbol{p}$ and subcarrier pairing $\boldsymbol{\pi}$.
- **P2:** Optimize the sum rate by varying subcarrier pairing $\boldsymbol{\pi}$ when fixing power allocation $\boldsymbol{p}$, source-node pairing $\boldsymbol{\varphi}$, and subcarrier assignment $\boldsymbol{\rho}$.
- **P3:** Optimize the sum rate by varying power allocation $\boldsymbol{p}$ when fixing subcarrier pairing $\boldsymbol{\pi}$, source-node pairing $\boldsymbol{\varphi}$, and subcarrier assignment $\boldsymbol{\rho}$.

### A. Source-Node Pairing and Subcarrier Assignment

Here, subcarriers are sequentially assigned based on the per-source-pair metric for each subcarrier. Here, we assume the subcarrier pairing $\pi_n = n$, and transmit power is equally allocated for each node among all assigned subcarriers.

Define the variable $\rho^{n,n}_{k,\varphi_k}(i)$ as the subcarrier assignment index indicating whether subcarrier $n$ will be assigned to source pair $(k,\varphi_k)$ for the $i$th iteration. Let $\Omega(i)$ be the set of selected source nodes and $m^{n,n}_{k,\varphi_k}(i)$ be the metric of source pair $(k,\varphi_k)$ if assigned with subcarrier $n$ for the $i$th iteration.

Then, the source-node pairing and subcarrier assignment phase involves four steps. First, for each subcarrier $n$, pair arbitrary two source nodes with each other, and find the best capacity among the minimum of source pairs, which are denoted by $\lambda_n := \max\limits_{(k,\varphi_k)} \min\{C^{n,n}_k, C^{n,n}_{\varphi_k}\}$. Second, find subcarrier permutation $\{\eta_i\}_{i\in N}$ among $\lambda_n$, such that $\lambda_{\eta_1} \geq \lambda_{\eta_2} \geq \ldots \geq \lambda_{\eta_N}$. We note that the given two steps are used to sort the subcarriers based on the best channel condition among all the source-pair candidates. Third, for the $i$th iteration, set a subcarrier index for source-pair candidates $(k,\varphi_k)$, i.e., $\rho^{\eta_i,\eta_i}_{k,\varphi_k}(i) = 1$, and assign subcarrier $\eta_i$ to source pair $(k,\varphi_k)^*$, such that this source pair has the largest value on metric, i.e., $(k,\varphi_k)^* = \arg\max\limits_{(k,\varphi_k)} \{m^{\eta_i,\eta_i}_{k,\varphi_k}(i)\}$. Metric $m^{\eta_i,\eta_i}_{k,\varphi_k}(i)$ is the total increase in the capacity of source pair $(k,\varphi_k)$ if assigned with subcarrier $\eta_i$, with an assumption that the transmit power is allocated equally over all assigned subcarriers. Thus, it can be expressed as

$$m^{\eta_i,\eta_i}_{k,\varphi_k}(i) = \sum_{n=1}^{N} \rho^{N,N}_{k,\varphi_k}(i) \min\left\{\overline{C^{N,N}_k}(i), \overline{C^{N,N}_{\varphi_k}}(i)\right\} - \sum_{n=1}^{N} \rho^{N,N}_{k,\varphi_k}(i-1) \min\left\{\overline{C^{N,N}_k}(i-1), \overline{C^{N,N}_{\varphi_k}}(i-1)\right\} \quad (19)$$

where $\overline{C^{n,n}_k}(i)$ are the transmission rate of source $k$ for the $i$th iteration with equal transmit power $\overline{p^n_k} = P_k / \sum_{n=1}^{N} \sum_{k\in\overline{\Omega}(i)} \rho^{n,n}_{k,\varphi_k}(i)$, $\overline{p^n_{\varphi_k}} = P_{\varphi_k} / \sum_{n=1}^{N} \sum_{\varphi_k\in\overline{\Omega}(i)\rho^{n,n}_{k,\varphi_k}(i)}$, and $\overline{p^n_R} = P_R/N$; here, set $\overline{\Omega}(i)$ is the temporary source-pair set, and $\overline{\Omega}(i) = \Omega(i-1)\bigcup(k,\varphi_k)$. Note that $\overline{\Omega}(i)$ is initialized as $\emptyset$, and all the source-pair metrics are updated after each subcarrier is assigned. $d$). Put the selected source pair $(k,\varphi_k)^*$ into $\Omega(i)$, and determine the source-node set $T_1$ and $T_2$ as

$$\begin{cases} T_1 = T_1 \cup k^* \quad T_2 = T_2 \cup \varphi^*_k & \text{if } |h^n_{k^*D}|^2 \geq \left|h^n_{\varphi^*_k D}\right|^2 \\ T_1 = T_1 \cup \varphi^*_k \quad T_2 = T_2 \cup k^* & \text{if } |h^n_{k^*D}|^2 < \left|h^n_{\varphi^*_k D}\right|^2 \end{cases} \quad (20)$$

where $T_1$ is the user set with a better channel condition, whereas $T_2$ is the worse case. From (13), we can obtain that the user in $T_2$ needs higher transmit power compared with the corresponding paired user in $T_1$.

The algorithm of source-node pairing and subcarrier assignment is summarized as Algorithm 1. It can be figured out that the complexity of the maximization process for all source-node pairs is $O(NM^2)$, and the sorting operation in subcarrier assignment has a complexity of $O(N\log N)$. Thus, the total complexity of Algorithm 1 is $O(NM^2 + N\log N)$.

**Algorithm 1 S1:** Source-Node Pairing and Subcarrier Assignment

1: **Initialize** Set $i = 0$, $\rho^{n,n}_{k,\varphi_k}(i) = 0$, $\Omega(i) = \emptyset$ for all $i$
2: **for** $n = 1, \ldots, N$ **do**
3: Pair any two source nodes.
4: Find the value $\lambda_n := \max\limits_{(k,\varphi_k)} \min\{C^{n,n}_k, C^{n,n}_{\varphi_k}\}$.
5: **end for**
6: Find the subcarrier permutation $\{\eta_i\}_{i\in N}$ such that $\lambda_{\eta_1} \geq \lambda_{\eta_2} \geq \ldots \geq \lambda_{\eta_N}$.
7: **for** $i = 1, \ldots, N$ **do**
8: Set $\rho^{\eta_i,\eta_i}_{k,\varphi_k}(i) = 1$ for each source pair $(k,\varphi_k)$.
9: Update metric $m_{k,\varphi_k{}^{\eta_i,\eta_i}}(i)$ through (19) for each source pair $(k,\varphi_k)$.
10: Find $(k,\varphi_k)^* = \arg\max\limits_{(k,\varphi_k)} \{m^{\eta_i,\eta_i}_{k,\varphi_k}(i)\}$.
11: Assign the selected subcarrier to source pair $(k,\varphi_k)^*$:

$$\rho^{\eta_i,\eta_i}_{k,\varphi_k}(i) = \begin{cases} 1 & \text{if } (k,\varphi_k) = (k,\varphi_k)^* \\ 0 & \text{if } (k,\varphi_k) \neq (k,\varphi_k)^* \end{cases}$$

12: For the selected source pair $(k,\varphi_k)^*$, set $\Omega(i) = \Omega(i)\bigcup(k,\varphi_k)^*$
13: Determine the source-node sets $T_1$ and $T_2$ as

$$\begin{cases} T_1 = T_1 \cup k^* \quad T_2 = T_2 \cup \varphi^*_k & \text{if } |h^n_{k^*D}|^2 \geq \left|h^n_{\varphi^*_k D}\right|^2 \\ T_1 = T_1 \cup \varphi^*_k \quad T_2 = T_2 \cup k^* & \text{if } |h^n_{k^*D}|^2 < \left|h^n_{\varphi^*_k D}\right|^2 \end{cases}.$$

14: **end for**

### B. Subcarrier Pairing

Having obtained $\boldsymbol{\varphi}^*$ and $\boldsymbol{\rho}^*$, we now determine the optimal subcarrier pairing. Define matrix $\mathbf{F} \in \mathbb{C}^{N\times N}$ containing the profit of assigning each subcarrier pair to the selected source pair as

$$\mathbf{F} = \begin{pmatrix} F_{1,1} & F_{1,2} & \cdots & F_{1,N} \\ F_{2,1} & F_{2,2} & \cdots & F_{2,N} \\ \vdots & \vdots & \ddots & \vdots \\ F_{N,1} & F_{N,2} & \cdots & F_{N,N} \end{pmatrix} \quad (21)$$

where $F_{n,n'}$ denotes the capacity for the selected source pair $(k,\varphi_k)^*$ on subcarrier pair $(n,n')$ when the transmit power is equally allocated for each node based on the assigned subcarrier number given earlier. Under the constraint that each subcarrier can pair only one subcarrier between two phases, we have to find an assignment that selects one element in each row and each column of matrix $\mathbf{F}$ such that the sum of profits is maximized. Therefore, this optimal subcarrier pairing problem is a linear assignment problem, which can be solved by efficient assignment algorithm such as the Hungarian method [23], which has complexity of $O(N^3)$.

### C. Power Allocation

Here, transmit power is optimally allocated when subcarrier is assigned and subcarrier is paired. In this case, the power optimization problem can be written as

$$\max_{p^n_k, p^{\pi_n}_R} \sum_{k\in T_2} \sum_{n=1}^{N} 2\rho^{n,\pi_n}_{k,\varphi_k} C^{n,\pi_n}_k \quad (22)$$

$$\text{s.t.} \sum_{n=1}^{N} \rho^{n,\pi_n}_{k,\varphi_k} p^n_k \leq P_k, k \in T_2 \quad (23a)$$

$$\sum_{k\in T_2} \sum_{n=1}^{N} \rho^{n,\pi_n}_{k,\varphi_k} p^{\pi_n}_R \leq P_R \quad (23b)$$

$$s^{n,\pi_n}_{k,\varphi_k} \leq C^{n,\pi_n}_k \leq \phi^{n,\pi_n}_{k,\varphi_k} \quad (23c)$$

where the set $T_i (i = 1, 2)$ is given by (20). This problem can be proven to be convex since the objective function is concave (see Appendix B) when $\boldsymbol{\rho}^*$, $\boldsymbol{\pi}^*$, and $\boldsymbol{\varphi}^*$ have been optimized. Moreover, the constraint functions (23a)–(23c) are affine. Hence, a duality gap, which is defined as the gap between the optimal solution of a primal problem and the solution of a dual problem, is zero [24]. Thus, in this paper, we solve P3 by the Lagrange dual decomposition method.

*1) Dual Problem Formulation:* Let $\boldsymbol{\gamma} = [\gamma_R, \gamma_1, \ldots, \gamma_K]$ denote nonnegative Lagrange multipliers. The Lagrangian associated with (22) can be expressed as (24), shown at the bottom of the page.

The corresponding dual function is

$$g(\boldsymbol{\gamma}) = \max_{\boldsymbol{p} \geq 0} L(\boldsymbol{p}, \boldsymbol{\rho}^*, \boldsymbol{\pi}^*, \boldsymbol{\varphi}^*). \tag{25}$$

The dual problem is given by

$$\min_{\boldsymbol{\gamma} \geq 0} g(\boldsymbol{\gamma}). \tag{26}$$

*2) Dual Decomposition and Solution:* We can rewrite dual problem $g(\boldsymbol{\gamma})$ in (26), which is also known as master problem, as

$$g(\boldsymbol{\gamma}) = \max_{p_k^n, p_R^{\pi_n} \geq 0} \sum_{k \in T_2} \sum_{n=1}^{N} \rho_{k,\varphi_k}^{n,\pi_n} \left(2C_k^{n,\pi_n} - \gamma_k p_k^n - \gamma_R p_R^{\pi_n}\right) + \sum_{k \in T_2} \gamma_k P_k + \gamma_R P_R. \tag{27}$$

Hence, the dual problem in (27) can be decomposed into several power allocation subproblems at the given dual points $\boldsymbol{\gamma}$. The subproblem can be expressed as

$$\max_{p_k^n, p_R^{\pi_n} \geq 0} L_{k,\varphi_k}^{n,\pi_n} \tag{28}$$

where $L_{k,\varphi_k}^{n,\pi_n}$ is

$$L_{k,\varphi_k}^{n,\pi_n} = \max_{p_k^n, p_R^{\pi_n}} 2C_k^{n,\pi_n} - \gamma_k p_k^n - \gamma_R p_R^{\pi_n}. \tag{29}$$

Applying the Karush–Kuhn–Tucker (KKT) condition [24] and considering constraint (23c), the optimal power allocation in high SNR can be expressed as

$$p_R^{\pi_n *} = \begin{cases} \min\left\{ \dfrac{\frac{2}{3}\frac{ad^2}{\gamma_R(ad+b)} - \frac{(ad+b)}{\left|h_{RD}^n\right|^2}}{d+bd+ad^2}, \Phi_R \right\}, & \dfrac{\left|h_{RD}^{\pi_n}\right|^2}{\gamma_R} \geq 2\dfrac{\left|h_{kD}^n\right|^2}{\gamma_k} \\ 0, & \dfrac{\left|h_{RD}^{\pi_n}\right|^2}{\gamma_R} < 2\dfrac{\left|h_{kD}^n\right|^2}{\gamma_k} \end{cases} \tag{30}$$

$$p_n^{n*} = \begin{cases} d\dfrac{\left|h_{RD}^{\pi_n}\right|^2}{\left|h_{kD}^n\right|^2} p_R^{\pi_n *}, & \dfrac{\left|h_{RD}^{\pi_n}\right|^2}{\gamma_R} \geq 2\dfrac{\left|h_{kD}^n\right|^2}{\gamma_k} \\ \min\left\{ \left(\dfrac{2}{3}\dfrac{1}{\gamma_k} - \dfrac{1}{\left|h_{kD}^n\right|^2}\right)^+, \Phi_k \right\}, & \dfrac{\left|h_{RD}^{\pi_n}\right|^2}{\gamma_R} < 2\dfrac{\left|h_{kD}^n\right|^2}{\gamma_k} \end{cases} \tag{31}$$

$$p_{\varphi k}^{n*} = \frac{\left|h_{kD}^n\right|^2}{\left|h_{\varphi_k D}\right|^2} p_k^{n*} \tag{32}$$

where $a = 2$, $b = 1 + |h_{kD}^n|^2/|h_{kR}^n|^2 + |h_{\varphi_k D}^n|^2/|h_{\varphi_k R}^n|^2$, $c = |h_{RD}^{\pi_n}|^2/|h_{kD}^n|^2\gamma_k/\gamma_R$, $d = 2ab + \sqrt{4a^2b^2 + 4ab(c-a)(b+1)}/2a(c-a)$, $\Phi_R = e^{3\phi_{k,\varphi_k}^{n,\pi_n}} - 1/d|h_{RD}^{\pi_n}|^2(ad + b/ad + b + 1)$, and $\Phi_k = e^{3\phi_{k,\varphi_k}^{n,\pi_n}} - 1/|h_{kD}^n|^2$. The detailed derivation is given in Appendix C.

An interesting phenomenon is observed in (30)–(32); if $|h_{RD}^{\pi_n}|^2\gamma_k < 2|h_{kD}^n|^2\gamma_R$, no transmit power is assigned to the relay node. In other words, network coding is not applied in this case, and transmit power at the source node is assigned by a water-filling method.

*3) Solution of the Master Problem:* The subgradient method [25] is used to solve the master problem. The update algorithm is given by

$$\gamma_k[j+1] = \left(\gamma_k(j) - \theta_k\left(P_k - \sum_{n=1}^{N} \rho_{k,\varphi_k}^{n,\pi_n} p_k^n\right)\right)^+ \tag{33}$$

$$\gamma_R[j+1] = \left(\gamma_R(j) - \theta_R\left(P_R - \sum_{n=1}^{N} p_R^{\pi_n}\right)\right)^+ \tag{34}$$

where $j$ is the iteration index. Variables $\theta_k$ and $\theta_R$ are step sizes for positive Lagrangian variables $\gamma_k$ and $\gamma_R$, respectively. To guarantee that the algorithm converges to the optimal solution, we set the step size as $1/\sqrt{j}$ [25], [26]. The minimization of the master problem is iteratively solved by (33) and (34) until convergence or the maximum iteration index is reached. The algorithm of power allocation can be summarized as Algorithm 2, where $L_{\max}$ is the maximum number of iterations, and $C_{\text{old}}$ and $C_{\text{new}}$ denote the sum capacity for the previous and current iteration indexes, respectively.

The computational complexity of solving the subproblems is $O(N)$. Let $T_1$ be the number of the subgradient method to update dual variables. Suggested by computational experience [25], $T_1$ is a polynomial function of the Lagrangian multipliers number. Therefore, the total computational complexity of the proposed resource-allocation algorithm (OPT) is $O(NM^2 + N\log N + N^3 + T_1 N)$, which is much less than that of solving the problem by exhaustive search, i.e., $O((C_M^2)^{N!} B^{(M+1)N})$. Here, $B$ is the maximum allowable bit cap.

$$L(\boldsymbol{p}, \boldsymbol{\rho}^*, \boldsymbol{\pi}^*, \boldsymbol{\varphi}^*) = \sum_{k \in T_2} \sum_{n=1}^{N} \frac{2}{3} \rho_{k,\varphi_k}^{n,\pi_n} \ln\left(1 + p_k^n |h_{kD}^n|^2 + \frac{p_k^n |h_{kD}^n|^2 p_R^{\pi_n} |h_{RD}^{\pi_n}|^2}{p_R^{\pi_n} |h_{RD}^{\pi_n}|^2 + p_R^{\pi_n}\left(\frac{|h_{kD}^n|^2 |h_{RD}^{\pi_n}|^2}{|h_{kR}^n|^2} + \frac{\left|h_{\varphi_k D}^n\right|^2 |h_{RD}^{\pi_n}|^2}{\left|h_{\varphi_k R}^n\right|^2}\right) + 2p_k^n |h_{kD}^n|^2}\right) + \sum_{k \in T_2} \gamma_k \left(P_k - \sum_{n=1}^{N} \rho_{k,\varphi_k}^{n,\pi_n} p_k^n\right) + \gamma_R \left(P_R - \sum_{k \in T_2} \sum_{n=1}^{N} \rho_{k,\varphi_k}^{n,\pi_n} p_R^{\pi_n}\right) \tag{24}$$

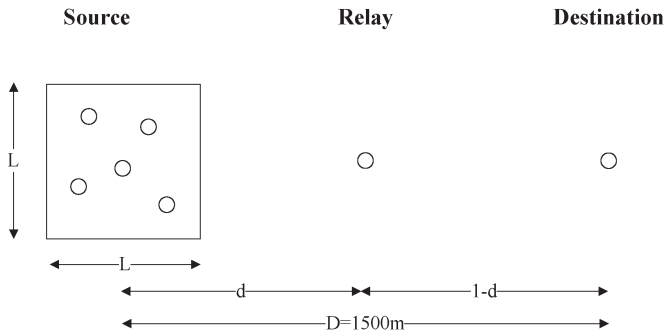


Fig. 3. Node location for simulation.

**Algorithm 2 S3:** Power Allocation

1: **Initialize** $L_{\max}$ and Lagrange multipliers $\{\boldsymbol{\gamma}\}$
2: **Initialize** sum rate $C_{\text{old}} = 0$ and set iteration index $j = 1$
3: Repeat
4: **for** each power-allocation subproblem **do**
5: Solve optimal $\boldsymbol{p}^*$ under given dual points $\{\boldsymbol{\gamma}\}$ when $\boldsymbol{\rho}^*$, $\boldsymbol{\pi}^*$, and $\boldsymbol{\varphi}^*$ have been optimized.
6: **end for**
7: Update the Lagrange multipliers $\boldsymbol{\gamma}$ using (33) and (34).
8: Calculate the sum rate $C_{\text{new}}$ and set $\varepsilon = |C_{\text{new}} - C_{\text{old}}|$
9: Update the sum rate $C_{\text{old}} = C_{\text{new}}$.
10: Until $\varepsilon < 0.00001$ or $j = L_{\max}$.

## IV. Simulation Results

Here, simulation results are provided to evaluate the performance of the proposed optimization algorithm OPT, as in Section III. To compare our algorithm with that without optimization, we further present simulation results for a baseline algorithm and three low-complexity suboptimal algorithms based on the proposed framework as follows. The first low-complexity suboptimal algorithm is OPT maximum per-user capacity (OPT-MPC). In OPT-MPC, each subcarrier is assigned to the source pair with the largest capacity among the minimum of all source pairs without considering per-user power constraints. The process of subcarrier paring and power allocation is operated as in Sections III-B and C, respectively. It can be observed that its complexity is $O(NM^2 + N^3 + T_1 N)$. The second algorithm is OPT fixing subcarrier pairing (OPT-FSP). First, pair the source node and then allocate the subcarrier as in Section III-A. Second, set the subcarrier in broadcast phase as that in relay phase, i.e., $\pi_n = n$. Third, allocate transmit power as in Section III-C. Its complexity is $O(NM^2 + N \log N + T_1 N)$. The third algorithm is OPT equal power allocation (OPT-EPA). Unlike OPT in Section III, in this algorithm, we allocate power equally. Compared with OPT, OPT-EPA does not need to update the dual variables. Hence, it has complexity of $O(NM^2 + N \log N + N^3)$. Similar to the previous low-complexity algorithms, the baseline algorithm operates as max per-user capacity, fixing subcarrier pairing, and equal power allocation.

In the simulation, we assume the location of the nodes shown in Fig. 3, where the source nodes are uniformly placed in a square region with $L$ as the length of side, and the distance between source cluster and destination is $D$. Each subcarrier occupies 25 kHz, and the number of subcarriers $N$ is 32. Moreover, we take the path-loss exponent to be 3.5. All the links in the simulation undergo independent fading, and Rayleigh fading on the each subcarrier is assumed.

Fig. 4 shows the average system capacity of the proposed OPT scheme and other schemes versus transmit power, where the number of source nodes is eight, $L$ is 500 m, and the relay node is located in the middle of the source cluster and the destination. We observe that the OPT scheme can achieve substantial improvement over baseline on the performance of the system sum rate, and it outperforms the baseline algorithm by 1.1 b/s/Hz on average when the transmit power is more than 0 dBm. In particular, the OPT can achieve about 33% improvement in sum capacity when the transmit power per node is about 5 dBm. Comparing OPT with three suboptimal algorithms, we can figure out that the performance gain between the OPT and OPT-EPA is the largest. It indicates that efficient power allocation among subcarriers can achieve better improvement in the spectral efficiency. It also revealed that the adaptive subcarrier assignment and subcarrier pairing can improve the average system capacity by 0.26 and 0.12 b/s/Hz on average, respectively. As shown in Fig. 4, the upper bound is also displayed in the same figure to be compared with the proposed schemes. The results indicate that the gap between the upper bound and the OPT scheme is negligible, which proves that the OPT scheme can achieve near-optimal solution. Moreover, the upper bound of our proposed scheme can improve throughput by 33% over the traditional scheme without network coding; therefore, the OPT scheme outperforms the traditional OFDM scheme without network coding.

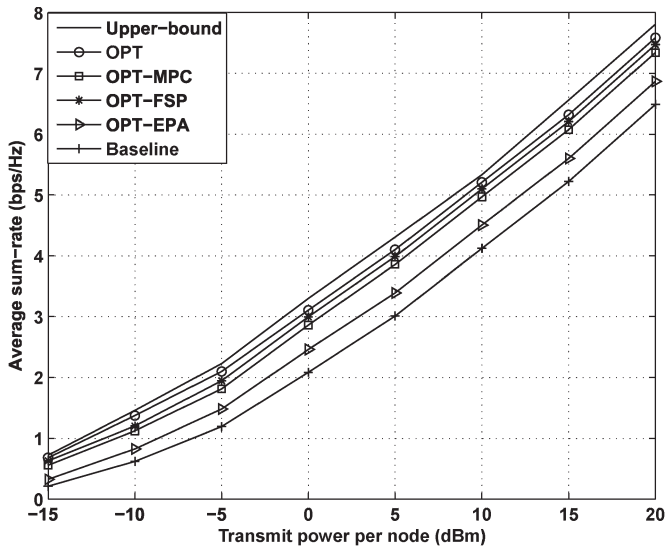


Fig. 4. Average sum rate versus transmit power with eight source nodes.

Fig. 5 shows the average capacity versus the number of source nodes when $P_k = P_R = 10$ dBm, and the node distribution is the same with Fig. 4. According to the simulation results, the same conclusion can be drawn that, for any source nodes number, the OPT scheme can obtain considerably gain over the baseline scheme, and compared with the three low-complexity schemes, OPT-FSP can achieve the largest gain. As shown in Fig. 5, it can be also seen that the performance of the proposed algorithms increases with the number of source nodes because multisource nodes can provide multiuser diversity.

Fig. 6 plots the average capacity versus the relay location when the number of source nodes is eight, and $P_k = P_R = 10$ dBm. In this simulation, we assume that source nodes are uniformly placed in a square region with 250 m as the length of side. Let $d$ be the distance ratio between the source–relay link and the source–destination link. For the proposed schemes, we can see that the optimal relay location is at around $d = 0.4$. It also can be observed that the OPT scheme can improve the system capacity, and the performance gain between OPT and OPT-FSP is decreasing when the relay node is moving to the source cluster or the destination.

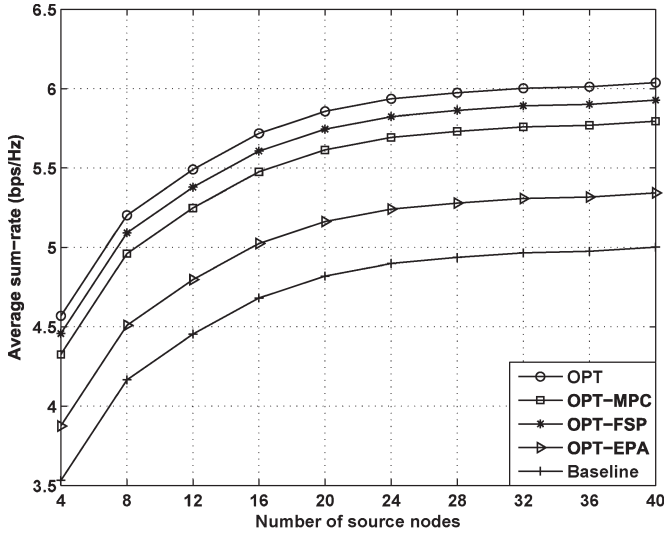


Fig. 5. Average sum rate versus source-node number when $P_k = P_R = 10$ dBm.

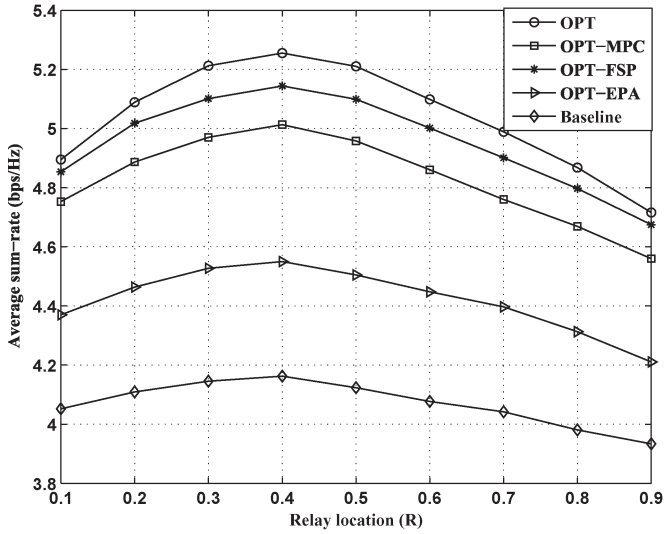


Fig. 6. Average sum rate versus relay location with eight source nodes when $P_k = P_R = 10$ dBm.

## V. Conclusion

In this paper, we have investigated the joint optimization problem of resource allocation in a multiuser OFDM-based uplink MARC with network coding. With the objective of maximizing the system sum rate, this problem jointly optimizes source node pairing, subcarrier assignment, subcarrier pairing, and power allocation under different resource constraints. The problem was solved through optimizing three separate subproblems in polynomial time: optimizing source node pairing and subcarrier assignment, assuming fixed subcarrier pairing and power allocation; optimizing subcarrier pairing by the Hungarian method assuming fixed subcarrier assignment and power allocation; and allocating the power by using dual decomposition method. Then, three low-complexity suboptimal algorithms were further proposed when only optimizing partial resource. The numerical results show that the proposed OPT scheme significantly outperform the baseline scheme and has only a small gap from the upper bound. Comparing the simulation results of OPT with that of the three suboptimal schemes, it can be observed that the suboptimal OPT-FSP scheme, which decouples the subcarrier pairing with subcarrier assignment and power allocation, performs closely to the OPT with less complexity.

## Appendix A
## Derivation of Minimum Mean Square Error Output Signal-to-Noise Ratio for (9) and (10)

The MMSE equalization matrix can be given by (see [21])

$$\mathbf{W}_{\mathrm{MMSE}} = (\mathbf{H}^{\mathbf{H}}\mathbf{H} + \mathbf{R})^{-\mathbf{1}}\mathbf{H}^{\mathbf{H}} \tag{35}$$

where $\mathbf{R}$ is the correlation matrix of equivalent noise $\mathbf{n}$ in (8), and $\mathbf{R}$ is given by

$$\mathbf{R} = \begin{bmatrix} 1 & 0 & 0 \\ 0 & 1 & 0 \\ 0 & 0 & \lambda \end{bmatrix} \tag{36}$$

where $\lambda = (\alpha_1 p_R^{\pi_n} |h_{RD}^n|^2 / p_k^n |h_{kR}^n|^2 + \alpha_2 p_R^{\pi_n} |h_{RD}^n|^2 / p_{\varphi_k}^n |h_{\varphi_k R}^n|^2 + 1)$.

Left multiplying the received signal vector $\mathbf{y}$ by $\mathbf{W}_{\mathrm{MMSE}}$, then the output SNR for user $k$ can be expressed as

$$\mathrm{SNR}_k = \frac{1}{[\mathbf{I} + \mathbf{H}^H \mathbf{R}^{-1} \mathbf{H}]_{k,k}^{-1}} - 1. \tag{37}$$

Substituting $\mathbf{H}$ and $\mathbf{R}$ into (37), we can obtain $\mathbf{H}^H \mathbf{R}^{-1} \mathbf{H}$ in (38), shown at the bottom of the page.

Therefore, the output SNR for source $S_k$ and $S_{\varphi_k}$ can be expressed, respectively, as

$$\mathrm{SNR}_k^{n,\pi_n} = \frac{(A+M+1)(B+N+1) - MN}{B+N+1} - 1 \tag{39}$$

$$\mathrm{SNR}_{\varphi_k}^{n,\pi_n} = \frac{(A+M+1)(B+N+1) - MN}{A+M+1} - 1 \tag{40}$$

where $A$, $B$, $M$, and $N$ are given in (9) and (10).

## Appendix B
## Derivation of the Concavity of (22)

It is easy to prove that (22) has the same concavity with the following equation:

$$f(x,y) = \ln\left(1 + x + \frac{xy}{ax+by}\right), \quad x > 0; \quad y > 0 \tag{41}$$

where $a$ and $b$ denote the nonnegative constant. Let $\nabla^2 f(x,y)$ be the Hessian matrix of $f$. Therefore, the first principal minors is given by

$$-\frac{a^4x^4 + 4a^3bx^3y + 2a^2bx\,(1+(2+3b)x)\,y^2}{2(ax+by)^2\,(ax(1+x)+(b+x+bx)y)^2} - \frac{2ab(b+x+3bx+2b^2x)y^3 + b^2(1+b)^2y^4}{2(ax+by)^2\,(ax\,(1+x)+(b+x+bx)\,y)^2} < 0. \tag{42}$$

$$\mathbf{H}^H\mathbf{R}^{-1}\mathbf{H} = \begin{bmatrix} p_k^n |h_{kD}^n|^2 + p_k^n p_R^{\pi_n} (\beta_1^n)^2 |h_{kR}^n|^2 |h_{RD}^n|^2 \lambda^{-1} & \sqrt{p_k^n p_{\varphi_k}^n}\, p_R^{\pi_n} \beta_1^n \beta_2^n h_{kR}^{n*} h_{RD}^{n*} h_{\varphi_k R}^n h_{RD}^n \lambda^{-1} \\ \sqrt{p_k^n p_{\varphi_k}^n}\, p_R^{\pi_n} \beta_1^n \beta_2^n h_{\varphi_k R}^{n*} h_{RD}^{n*} h_{\varphi_k R}^n h_{RD}^n \lambda^{-1} & p_{\varphi_k}^n \left|h_{\varphi_k D}^n\right|^2 + p_{\varphi_k}^n p_R^{\pi_n} (\beta_2^n)^2 \left|h_{\varphi_k R}^n\right|^2 |h_{RD}^n|^2 \lambda^{-1} \end{bmatrix} \tag{38}$$

The second principal minors can be obtained as

$$\frac{2abx^2(ax+y+by)^2}{(ax+by)^2\left(ax(1+x)+(b+x+bx)y\right)^3}>0. \tag{43}$$

Therefore, the matrix $\nabla^2 f(x,y)$ is negative definite. With the help of [24], the concavity of (22) is proven.

## Appendix C
## Derivation of the Optimal Solution for (30)–(32)

For simplicity, we first rewrite (29) as

$$L_{k,\varphi_k}^{n,\pi_n}=\frac{2}{3}\ln\left(1+x+\frac{xy}{ax+by}\right)-\frac{\gamma_k x}{|h_{kD}^n|^2}-\frac{\gamma_R y}{|h_{RD}^{\pi_n}|^2} \tag{44}$$

where $a=2$, $b=1+|h_{kD}^n|^2/|h_{kR}^n|^2+|h_{\varphi_k D}^n|^2/|h_{\varphi_k R}^n|^2$, $c=|h_{RD}^{\pi_n}|^2/|h_{kD}^n|^2\gamma_k/\gamma_R$, $x=p_k^n|h_{kD}^n|^2$, and $y=p_R^{\pi_n}|h_{RD}^{\pi_n}|^2$. By applying the KKT condition at the given dual point, we can yield

$$\frac{2}{3}\frac{(ax+by)^2+by^2}{((1+x)(ax+by)+xy)(ax+by)}=\frac{\gamma_k}{|h_{kD}^n|^2} \tag{45}$$

$$\frac{2}{3}\frac{ax^2}{((1+x)(ax+by)+xy)(ax+by)}=\frac{\gamma_R}{|h_{RD}^{\pi_n}|^2}. \tag{46}$$

Combining (45) and (46), we can obtain that

$$\frac{|h_{kD}^n|^2 p_k^n}{|h_{RD}^{\pi_n}|^2 p_R^{\pi_n}}=d \tag{47}$$

where $d=2ab+\sqrt{4a^2b^2+4ab^3(c-a^3)^3(b+1^3)}/2a^3(c-a^3)$.

To ensure that $x$ and $y$ are positive, we have $|h_{RD}^{\pi_n}|^2\gamma_k\geq 2|h_{kD}^n|^2\gamma_R$. Submitting (47) into (45) and (46), the optimal power at the relay node is given by

$$p_R^{\pi_n *}=\begin{cases}\dfrac{\left(\frac{2}{3}\frac{ad^2}{\gamma_R(ad+b)}-\frac{(ad+b)}{|h_{RD}^n|^2}\right)}{d+bd+ad^2}, & |h_{RD}^{\pi_n}|^2\gamma_k\geq 2|h_{kD}^n|^2\gamma_R\\ 0, & |h_{RD}^{\pi_n}|^2\gamma_k<2|h_{kD}^n|^2\gamma_R.\end{cases} \tag{48}$$

When no power is allocated to the relay node, the power at source node should follow the water-filling method. Therefore, the optimal power at the source node is given by

$$p_k^{n*}=\begin{cases}d\frac{|h_{RD}^{\pi_n}|^2}{|h_{kD}^n|^2}p_R^{\pi_n *}, & |h_{RD}^{\pi_n}|^2\gamma_k\geq 2|h_{kD}^n|^2\gamma_R\\ \left(\frac{2}{3}\frac{1}{\gamma_k}-\frac{1}{|h_{kD}^n|^2}\right), & |h_{RD}^{\pi_n}|^2\gamma_k<2|h_{kD}^n|^2\gamma_R.\end{cases} \tag{49}$$

Combining the constraints (18a), (44), and (47), we can yield

$$s_{k,\varphi_k}^{n,\pi_n}\leq\frac{1}{3}\ln\left(1+x+\frac{xy}{ax+by}\right)\leq\phi_{k,\varphi_k}^{n,\pi_n} \tag{50}$$

$$\frac{x}{y}=d. \tag{51}$$

Then, the optimal power allocation is restrained by

$$\frac{e^{3s_{k,\varphi_k}^{n,\pi_n}}-1}{d|h_{RD}^{\pi_n}|^2}\left(\frac{ad+b}{ad+b+1}\right)\leq p_R^{\pi_n *}\leq\frac{e^{3\phi_{k,\varphi_k}^{n,\pi_n}}-1}{d|h_{RD}^{\pi_n}|^2}\left(\frac{ad+b}{ad+b+1}\right). \tag{52}$$

For simplicity, we assume that the lower bound $s_{k,\varphi_k}^{n,\pi_n}$ is 0 nat/Hz. From (48), (49) and (52), the optimal power is determined by

$$p_R^{\pi_n *}=\begin{cases}\min\left\{\dfrac{\frac{2}{3}\frac{ad^2}{\gamma_R(ad+b)}-\frac{(ad+b)}{|h_{RD}^n|^2}}{d+bd+ad^2},\Phi_R\right\}, & \frac{|h_{RD}^{\pi_n}|^2}{\gamma_R}\geq 2\frac{|h_{kD}^n|^2}{\gamma_k}\\ 0, & \frac{|h_{RD}^{\pi_n}|^2}{\gamma_R}<2\frac{|h_{kD}^n|^2}{\gamma_k}\end{cases} \tag{53}$$

$$p_n^{n*}=\begin{cases}d\frac{|h_{RD}^{\pi_n}|^2}{|h_{kD}^n|^2}p_R^{\pi_n *}, & \frac{|h_{RD}^{\pi_n}|^2}{\gamma_R}\geq 2\frac{|h_{kD}^n|^2}{\gamma_k}\\ \min\left\{\left(\frac{2}{3}\frac{1}{\gamma_k}-\frac{1}{|h_{kD}^n|^2}\right)^+,\Phi_k\right\}, & \frac{|h_{RD}^{\pi_n}|^2}{\gamma_R}<2\frac{|h_{kD}^n|^2}{\gamma_k}\end{cases} \tag{54}$$

where $\Phi_R=e^{3\phi_{k,\varphi_k}^{n,\pi_n}}-1/d|h_{RD}^{\pi_n}|^2(ad+b/ad+b+1)$, and $\Phi_k=e^{3\phi_{k,\varphi_k}^{n,\pi_n}}-1/|h_{kD}^n|^2$.

The proof of the optimal solution $\boldsymbol{p}*$ is done.

## References


[1] R. Pabst, B. Walk, and D. Schultz, "Relay-based deployment concepts for wireless and mobile broadband radio," *IEEE Commun. Mag.*, vol. 42, no. 9, pp. 80–89, Sep. 2004.

[2] J. N. Laneman, D. N. C. Tse, and G. W. Wornell, "Cooperative diversity in wireless networks: Efficient protocols and outage behavior," *IEEE Trans. Inf. Theory*, vol. 50, no. 12, pp. 3062–3080, Dec. 2004.

[3] R. Ahlswede, N. Cai, S.-Y. R. Li, and R. W. Yeung, "Network information flow," *IEEE Trans. Inf. Theory*, vol. 46, no. 4, pp. 1204–1216, Jul. 2000.

[4] S.-Y. R. Li, R. W. Yeung, and N. Cai, "Linear network coding," *IEEE Trans. Inf. Theory*, vol. 49, no. 2, pp. 371–381, Feb. 2003.

[5] M. Peng, C. Yang, Z. Zhao, W. Wang, and H. Chen, "Cooperative network coding in relay-based IMT-Advanced systems," *IEEE Commun. Mag.*, vol. 50, no. 4, pp. 76–84, Apr. 2012.

[6] X. Bao and J. Li, "Adaptive network coded cooperation (ANCC) for wireless relay networks: Matching code-on-graph with network-on-graph," *IEEE Trans. Wireless Commun.*, vol. 7, no. 2, pp. 574–583, Feb. 2008.

[7] Z. Ding, T. Wang, M. Peng, W. Wang, and K. K. Leung, "On the design of network coding for multiple two-way relaying channels," *IEEE Trans. Wireless Commun.*, vol. 10, no. 6, pp. 1820–1832, Jun. 2011.

[8] M. Ju and I.-M. Kim, "Selection with ANC and TDBC protocol in bidirectional relay networks," *IEEE Trans. Commun.*, vol. 58, no. 12, pp. 3500–3511, Dec. 2010.

[9] Z. Yi, M. Ju, and I.-M. Kim, "Outage probability and optimum combining for time division broadcast protocol," *IEEE Trans. Wireless Commun.*, vol. 10, no. 5, pp. 1362–1367, May 2011.

[10] Y. Chen, S. Kishore, and J. Li, "Wireless diversity through network coding," in *Proc. IEEE WCNC*, Mar. 2006, pp. 1681–1686.

[11] M. Peng, H. Liu, W. Wang, and H.-H. Chen, "Cooperative network coding with MIMO transmission in wireless decode-and-forward relay networks," *IEEE Trans. Veh. Technol.*, vol. 59, no. 7, pp. 3577–3588, Sep. 2010.

[12] P. Tan, C. Ho, and S. Sun, "OFDM modulated cooperative multiple-access channel with network-channel coding," *IEEE Trans. Wireless Commun.*, vol. 11, no. 2, pp. 604–613, Feb. 2012.

[13] M. Kaneko, K. Hayashi, P. Popovski, K. Ikeda, and R. Prasad, "Amplify-and-forward cooperative diversity schemes for multi-carrier systems," *IEEE Trans. Wireless Commun.*, vol. 7, no. 5, pp. 1845–1850, May 2008.

[14] Y. Li, W. Wang, J. Kong, and M. Peng, "Subcarrier pairing for amplify-and-forward and decode-and-forward OFDM relay links," *IEEE Commun. Lett.*, vol. 13, no. 4, pp. 209–211, Apr. 2009.

[15] W. Dang, M. Tao, H. Mu, and J. Huang, "Subcarrier-pair based resource allocation for cooperative multi-relay OFDM sytems," *IEEE Trans. Wireless Commun.*, vol. 9, no. 5, pp. 1640–1649, May 2010.

[16] L. Song, "Relay selection for two-way relaying with amplify-and-forward protocols," *IEEE Trans. Veh. Technol.*, vol. 60, no. 4, pp. 1954–1959, May 2011.

[17] C. K. Ho, R. Zhang, and Y. C. Liang, "Two-way relaying over OFDM: Optimized tone permutation and power allocation," in *Proc. IEEE ICC*, Beijing, China, May 2008, pp. 3908–3912.

[18] Y. Liu and M. Tao, "Optimal channel and relay assignment in OFDM-based multi-relay multi-pair two-way communication networks," *IEEE Trans. Commun.*, vol. 60, no. 2, pp. 317–321, Feb. 2012.

[19] H. Zhang, Y. Liu, and M. Tao, "Resource allocation with subcarrier pairing in OFDMA two-way relay networks," *IEEE Wireless Commun. Lett.*, vol. 1, no. 2, pp. 61–64, Apr. 2012.
[20] M. Peng, Z. Zhao, X. Xie, and W. Wang, "A network coded interference coordination scheme in cellular relay systems," *IEEE Commun. Lett.*, vol. 16, no. 5, pp. 688–690, May 2012.
[21] Y. Jiang, M. Varanasi, and J. Li, "Performance analysis of ZF and MMSE equalizers for MIMO systems: An in-depth study of the high SNR regime," *IEEE Trans. Inf. Theory*, vol. 57, no. 4, pp. 2008–2026, Apr. 2011.
[22] X. Zhang and S. Y. Kung, "Capacity analysis for parallel and sequential MIMO equalizers," *IEEE Trans. Signal Process.*, vol. 51, no. 11, pp. 2989–3002, Nov. 2003.
[23] H. Khun, "The Hungarian method for the assignment problems," *Naval Res. Logist. Quart.*, vol. 2, no. 1/2, pp. 83–97, 1955.
[24] S. Boyd and L. Vandenberghe, *Convex Optimization*. Cambridge, U.K.: Cambridge Univ. Press, 2004.
[25] S. Boyd and A. Mutapcic, "Subgradient methods," Standford Univ., Stanford, CA, USA, Winter 2006, notes for EE364.
[26] W. Yu and R. Lui, "Dual method for nonconvex specturm optimization of multicarrier systems," *IEEE Trans. Commun.*, vol. 54, no. 7, pp. 1310–1322, Jul. 2006.

# On Hybrid Overlay–Underlay Dynamic Spectrum Access: Double-Threshold Energy Detection and Markov Model

Xueyuan Jiang, *Student Member, IEEE*,
Kai-Kit Wong, *Senior Member, IEEE*,
Yangyang Zhang, *Member, IEEE*, and
David Edwards, *Senior Member, IEEE*

***Abstract*—In this correspondence, we propose a hybrid strategy that combines overlay and underlay dynamic spectrum access (DSA) schemes. Utilizing a double-threshold energy detection method, unlicensed or secondary users (SUs) can switch between full- and partial-access modes dynamically. A Markov chain model is developed to derive performance metrics for evaluating the proposed strategy. Numerical results show that the proposed strategy can greatly improve the system interfering probability performance. In addition, SUs can adjust the access probability of partial-access mode to tradeoff between throughput and interfering probability performance.**

***Index Terms*—Cognitive radio (CR), double-threshold energy detection, dynamic spectrum access (DSA), hybrid access.**

Manuscript received June 13, 2012; revised October 12, 2012 and February 25, 2013; accepted April 7, 2013. Date of publication April 16, 2013; date of current version October 12, 2013. This work was supported in part by the Guangdong Science and Technology Plan Project under Grant 2011A010801009, by the Shenzhen Science and Technology Plan Project under Grant JC201005280649A, by the Guangdong High-End Electronic Information Special in Strategic Emerging Industry Development Plan under Grant 2012556019, and by the Introduction of Innovative R&D Team Program of Guangdong Province under Grant 2009010005. The review of this paper was coordinated by Dr. H. Jiang.

X. Jiang and D. Edwards are with the Department of Engineering Science, University of Oxford, Oxford OX1 3PJ, U.K. (e-mail: xueyuan.jiang@eng.ox.ac.uk; david.edwards@eng.ox.ac.uk).

K.-K. Wong is with the Department of Electronic and Electrical Engineering, University College London, London WC1E 7JE, U.K. (e-mail: kai-kit.wong@ucl.ac.uk).

Y. Zhang is with the Shenzhen Key Laboratory of Artificial Microstructure Design and the Guangdong Key Laboratory of Meta-RF Microwave Radio Frequency, Kuang-Chi Institute of Advanced Technology, Shenzhen 518000, China (e-mail: yangyang.zhang@kuang-chi.org).

Color versions of one or more of the figures in this paper are available online at http://ieeexplore.ieee.org.

Digital Object Identifier 10.1109/TVT.2013.2258360

## I. Introduction

Dynamic spectrum access (DSA) [1] and cognitive radio (CR) [2] have been proposed and become the enabling technologies to more intelligently allocate the spectrum to users. Under the framework of DSA, unlicensed or secondary users (SUs) can share the spectrum with licensed or primary users (PUs). With CR capabilities, SUs are able to observe the spectrum activity and dynamically adjust their operating parameters to access vacant spectrum spaces while making sure that no harmful interference is caused to the PUs.

Hierarchical overlay and underlay access schemes have been shown to achieve a good tradeoff between spectrum efficiency and interference control for DSA [1]. For overlay access, SUs perform spectrum sensing to obtain the current spectrum occupancy information and access the spectrum not used by PUs opportunistically. Reliable spectrum sensing algorithms and an optimal sensing–access mechanism have been widely addressed in [3]–[5]. For underlay access schemes, by constraining the transmission power of SUs and minimizing interference to PUs, SUs can access the spectrum even if PUs are active. Efficient power allocation and adaptive interference threshold constraint methods have been presented in [6], [7].

Interference tolerance of PUs is ignored for overlay access, whereas the possibility for SUs to transmit at higher power when PUs are inactive is forbidden for underlay access. Therefore, mixed or hybrid strategies are preferred to improve spectrum efficiency. In [8], a hybrid CR system was proposed, where the system is normally working in overlay mode but may switch to underlay mode based on a probabilistic control method for the departure rate of SU transmitters. In addition, Chakravarthy *et al.* [9] designed a hybrid overlay–underlay waveform to enable a soft decision in CR and to exploit both unused and underused spectrum resources. Later, Khoshkholgh *et al.* [10] further considered the interference- or power-constrained spectrum sharing system and proposed a mixed access strategy in which SUs attempt to transmit with a predefined probability to ensure the overall interference under a certain threshold.

In this correspondence, we propose a hybrid full–partial access strategy for DSA. A double-threshold energy detection method is proposed to identify the PU's operating location. Based on observations, SUs dynamically switch between full- and partial-access modes. A Markov chain model is developed to analyze the proposed strategy. Performance metrics such as the throughput of SUs and interfering probability to PU will be derived. Our main contribution is that we jointly model and analyze spectrum sensing in the physical (PHY) layer with hybrid access in the multiple-access control (MAC) layer.

## II. System Model

### A. Network Model

We consider a DSA network consisting of $N$ primary channels and a number of PUs and SUs. To make our analysis tractable, we focus on a single primary channel with bandwidth $W$. Our objective is to study the achievable throughput and the average interfering probability on this channel by introducing the SUs. In particular, there is a pair of SU transmitter (Tx) and receiver (Rx) in a given area of interest. From the SU's viewpoint, a PU transmitter (Tx) and receiver (Rx) may appear at random locations in the area with radius $D_1$, as shown in Fig. 1. We also specify the shaded region within radius $D_2$ as Region 2 in the figure, and its operational meaning will be explained later. We assume that a PU can be referred to as a pair of PU Tx and Rx, which are located in the same region (Region 1 or Region 2), but their locations are independent and randomly distributed within that region.